ACS Photonics

Article

pubs.acs.org/journal/apchd5

Large Area Plasmonic Color Palettes with Expanded Gamut Using Colloidal Self-Assembly

Liancheng Wang,[†] Ray Jia Hong Ng,[†,‡] Saman Safari Dinachali,[†] Mahsa Jalali,[†] Ye Yu,[†] and Joel K. W. Yang*[,†,‡]

[†]Engineering Product Development, Singapore University of Technology and Design, 8 Somapah Road, Singapore 487372

[‡]Institute of Materials Research and Engineering (IMRE), A*STAR, 2 Fusionopolis Way, Innovis, Singapore 138634

Supporting Information

ABSTRACT: Optical resonances in metallic nanostructures are promising in enabling high-resolution plasmonic color prints, color filters, and in rendering colors for plastic consumer products. However, nanostructure patterning approaches have relied on charged-particle beam lithography, with limited throughput. For the purpose of visually evaluating colors spanning a large parameter space, it is important to develop a rapid and cost-effective approach to patterning large areas. The speed at which the parameter space is explored experimentally needs to be comparable to the time it takes to run full electromagnetic simulations. Here, we used a bottom-up approach to cost-effectively create periodic nanostructures on centimeter-scale samples. Upon further processing, this approach produced more complex geometries, such as rings and domes, compared to the standard structures consisting of metal disks. By adjusting various geometric parameters, vivid colors with an expanded gamut were obtained.

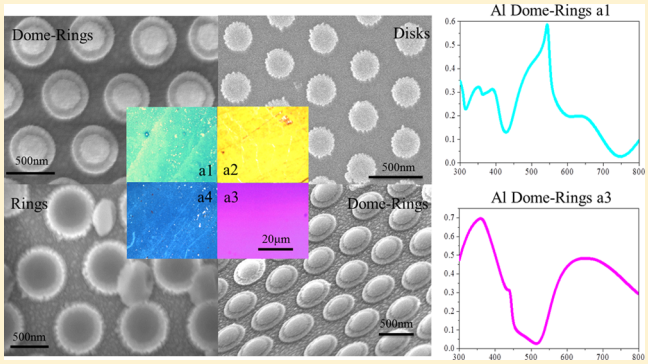

KEYWORDS: *plasmonic color, aluminum, polystyrene, colloidal self-assembly*

Plasmon resonances in metal nanostructures are promising as color-rendering elements with several advantages over dye-based colorants. The inherent characteristics of localized plasmon resonances are their strong field confinement and geometry-dependent color control that enable lithographically defined color prints with resolutions beyond the optical diffraction limit.[1,2] Examples of its applications include ∼100000 dots-per-inch resolution printing,[2,3] display,[4,5] data archival, macroscopic color holograms,[6] color filters,[7,8] polarizers,[9] and three-dimensional color stereoscopic prints.[10] Recently, aluminum (Al) has proven to be a suitable material due to its natural abundance, self-limiting protective oxide, and tolerance to dimensional variation,[4,7,11−14] despite its limited gamut. Efforts to increase the gamut and color saturation include plasmonic color mixing[4] and the use of far-field diffractive effects.[11] Additionally, large-scale patterning of plasmonic color prints have relied on electron-beam lithography, which could be time-consuming for centimeter-scale prints.[7−9,2−5] A study that explores a method of rapidly creating large-area plasmonic colors is therefore needed.

Here we use the well-known colloidal self-assembly approach[15−18] to pattern large areas of plasmonic color. Furthermore, we demonstrate the use of this method for exploring the parameter space and obtaining new nanostructure designs that result in a wider color gamut. In addition to the previously reported structural configuration consisting of metal disks raised above a holey back reflector (Disks),[2,4,10] this approach enables complex structures such as dome-ring-back reflector (Dome-Rings), and rings above a holey back reflector (Rings) design. This approach proves to be valuable in the rapid evaluation of plasmonic colors spanning a large parameter space, for example, pitch, diameter, height, and nanostructure geometry. The self-assembly process takes only ∼3 hours to obtain 20 pieces of ∼1.5 cm × 1.5 cm sized sample with systematically varied pitches, heights, and diameters. The underlying resonant modes were selectively investigated through simulations. The expanded gamut achieved is a step closer to achieving full vibrant plasmonic colors. This report provides a convenient and cost-effective approach to achieving a range of plasmonic nanostructure designs for optical evaluation.

RESULTS AND DISCUSSION

Figure 1 illustrates the unit cells of the structures under consideration, that is, Disks, Dome-Rings, and Rings that form a hexagonal lattice. The right panel shows the compilation of colors obtained from these structures on the 1931 CIE color space. For comparison, we overlay the gamut of representative commercial LCD and OLED technologies.[19,20] In the range of parameters explored (more details in the following), the

Received: December 17, 2015
Published: February 19, 2016

DOI: 10.1021/acsphotonics.5b00725
ACS Photonics 2016, 3, 627−633

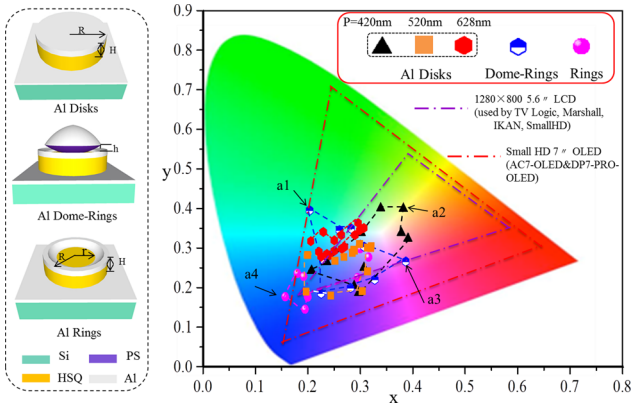

Figure 1. Schematic of the plasmonic nanostructure designs achieved using the colloidal polystyrene (PS) self-assembly approach (left), and their corresponding colors plotted on the 1931 CIE map (right). Unit cells of Disks, Dome-Rings, and Rings of a hexagonal close-packed array are shown, after pattern transfer into a hydrogen silsesquioxane (HSQ) layer and deposition of 15 nm thick aluminum (Al) to support plasmon resonances. The radius (R), inner radius (r), height (H), and pitch (P) of the structures were varied in the fabrication process and the resulting colors were measured. The parameters were varied in the range of R = 90−300 nm, H = 50−120 nm, $R - r$ = 50−150 nm, and P = 420−628 nm. Parameters that generated especially vibrant colors as viewed under normal illumination are indicated by the points a1−a4. For comparison, we overlaid the gamut of commercial LCD (used by TV Logic, Marshall, IKAN, SmallHD), and OLED (AC7-OLED and DP7-PRO-OLED) on the CIE map.

fabricated structures show limited saturation in the green to red region, but highly saturated colors in the blue region. Specifically, the 420 nm pitch Disks have a gamut that occupies a large fraction of that of the LCD, spanning from light blue to pink to yellow. The 628 nm pitch based Disks have a smaller gamut in comparison, but produces more saturated cyans compared to LCDs. With the Rings nanostructure design, the blue colors achieved are beyond that of the OLED's gamut. This suggests that saturated colors beyond the capability of existing display technologies can be achieved. The Al Dome-Rings structure extends the color gamut to the boundary of the OLED's gamut in the green region. The obtained gamut shows some unique colors occupying a broader gamut when contrasted with previous reports.[4,7,11,13]

FABRICATION PROCESS

The specific fabrication process of Disks, Dome-Rings, and Rings is illustrated in Figure 2a. Hydrogen silsesquioxane (HSQ, Dow Corning XR-1541) was spin-coated onto silicon substrates. The height of the dielectric spacer was controlled by varying the thickness of HSQ (from 50 to 120 nm), controlled by the spin-coating speed. Monolayer polystyrene spheres (PS, from microParticles GmbH) were self-assembled on a liquid/gas interface and transferred onto the HSQ-coated samples using the Langmuir−Blodgett approach.[15,16] The pitch of the resulting patterns was determined by the diameter of the PS particles. Reactive-ion etching (RIE, O_2 20 sccm, 30 W, Femto Science Inc.) was used to reduce the size of PS spheres to the

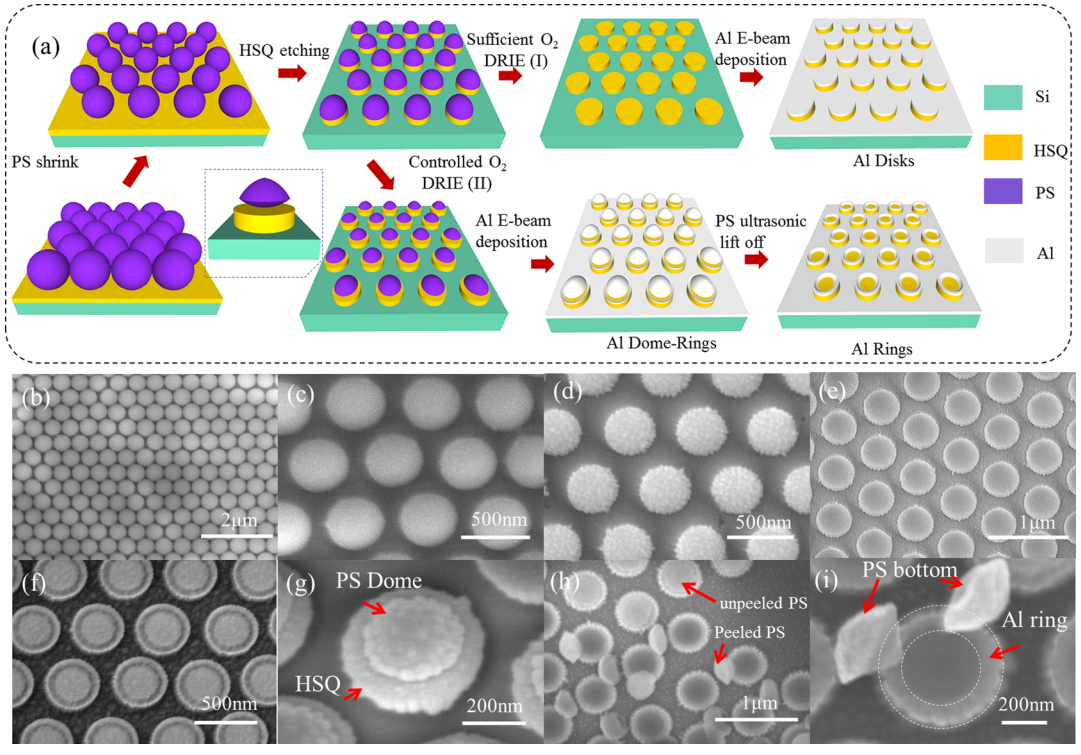

Figure 2. (a) Schematic of the fabrication process of the Disks, Al Dome-Rings, and Rings, including HSQ spin coating and PS monolayer transfer; PS size shrinkage; HSQ etching; removal of PS using two routes: route I, O_2 RIE process to completely remove the top PS and obtain the Disks; or route II, O_2 DRIE to further shrink the PS spheres to obtain Al Dome-Rings; Rings are obtained by ultrasonic removal of the PS from the Al Dome-Rings. SEM images are shown for (b) self-assembled monolayer PS with 520 nm pitch; (c) PS size shrinkage by RIE process; (d) HSQ etching with the top PS as the etching mask; (e) Disks; (f) Al Dome-Rings with (R, r) = (215, 165) nm, with the unit shown by enlarged and tilted SEM in (g); (h) Rings with the top PS domes partially peeled off after sonication, (i) High-magnification tilted SEM image of a single Ring structure with partially removed domes.

DOI: 10.1021/acsphotonics.5b00725
ACS Photonics 2016, 3, 627−633

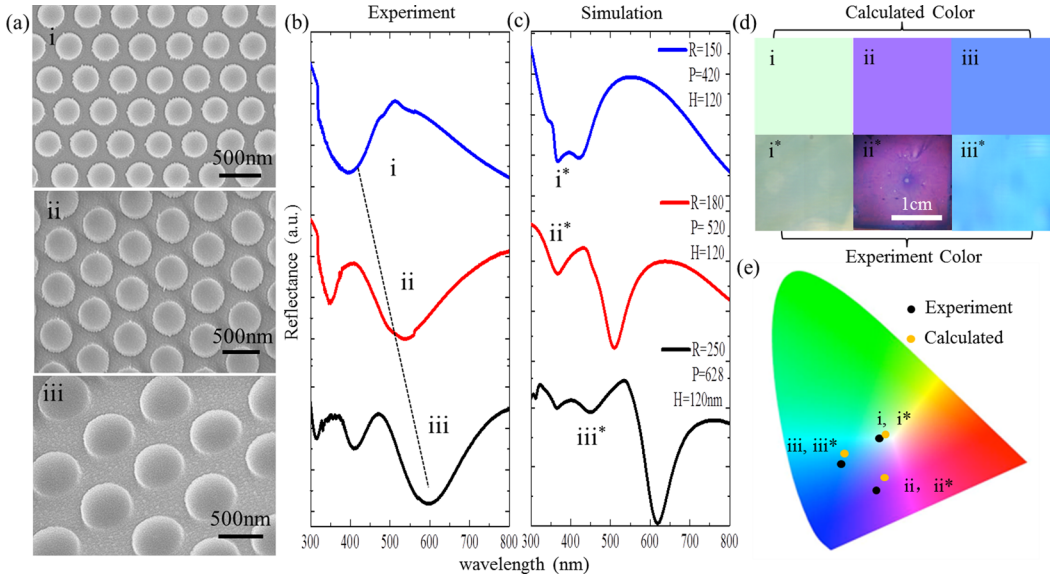

Figure 3. (a) SEM images of Disks with H = 120 nm, (P, R) = (420, 150) nm (a, i), (520, 180) nm (a,ii), (628, 250) nm (a,iii); (b, c) Experimental and simulated reflectance spectra of the Disks corresponding to (a, i), (a,ii), and (a,iii); (d) Experimental and simulated colors for the Disks in (a, i), (a,ii), and (a,iii); (e) Corresponding chromaticity coordinates from the spectra in (b) and (c).

desired diameter while keeping the pitch unchanged. The measured lateral shrink rate of the particles was ∼25 nm/min. A deep reactive-ion etcher (DRIE, CHF_3 25 sccm, Ar 40 sccm, Oxford Instruments) was used to transfer the pattern into the HSQ layer using the size-reduced PS spheres as the etch mask. HSQ post arrays were obtained by removing the PS spheres through an additional O_2 DRIE process (Figure 2, route I, 30 W, 20 sccm O_2, 150 s, process temperature 10 °C), whereas a structure with PS spheres on HSQ posts was obtained via a short O_2 DRIE process (Figure 2, route II, 30 W, 20 sccm O_2, 30−80 s, process temperature 10 °C). A 15 nm thick layer of Al (0.01 nm/s, ∼40 W) was deposited using an E-beam evaporator (Kurt J. Lesker Company), to create Disks structure. The Dome-Rings structures were obtained via route II. To create the Rings structure, samples were sonicated in DI water for ∼30 min to detach the Al dome. Multiple structural parameters, for example, pitch (particle diameter), height of structures (HSQ thickness), diameter of structures (O_2 RIE treatment time), and ring width (second O_2 DRIE treatment time), can be systematically varied to tailor the reflectances. The width (R − r) of the Rings is determined by the RIE process duration (which determines the outer radius R) and the O_2 DRIE process duration (which determines the inner radius r). For the Al Dome-Rings, the spacer distance between the top PS dome and the bottom ring (left panel in Figure 1), H, is dependent on the deformation of the PS spheres. For PS spheres with 420 nm pitch, H ranged from 0 to 50 nm, as indicated from Figure 2h,i.

Figure 2b−i shows representative scanning electron microscope (SEM) images displaying different stages of the fabrication process for creating periodic Disk structures with a pitch of 520 nm. PS sphere monolayer crystal assemblies with pitch P = 628, 520, and 420 nm were chosen. The self-assembled monolayer of PS spheres was closely packed (Figure 2b). The RIE process shrinks the PS anisotropically, causing the PS structure to deviate from a sphere (Figure 2c). The diameter after RIE is uniform across the entire array of particles. Our proposed process shows high reproducibility and reliability with over ∼100 μm range ordering (Figure S2). PS spheres function as the DRIE etch mask, for pattern transfer to the underlying HSQ posts (Figures 2d and S1(b)). Surface irregularities and roughness appeared when the particles were etched to roughly half of their original size (Figure S1(a)),[21] due likely to random redeposition of etch-resistant material around the particles. After size reduction, the PS spheres act as etch masks for DRIE pattern transfer into HSQ posts (Figures 2d and S1(b)). With further size reduction, the integrity of PS as the etch mask is severely reduced. In this paper, we investigated only colors arising from particles that experienced a size reduction of no greater than 80% of its original size (Figure S1(b)).

After the pattern transfer into HSQ, Disks were obtained by O_2 plasma DRIE to remove the PS particles (∼120 s, 30 W, O_2 20 sccm), followed by electron-beam evaporation of Al, as shown in Figure 2e. Figure 2f shows Al Dome-Rings with P = 520 nm and (R, r) = (215, 165) nm and Figure 2g shows the enlarged and tilted SEM image of a single Dome-Rings structure. The line between the dome on PS and its ring below indicates the gap of 0−50 nm between the dome and ring structures. Figure 2h shows the SEM image of the structure with the top PS incompletely removed after sonication to illustrate the side view of the domes. The exposed underlying Rings and the detached PS were clearly observed. A high-magnification SEM image of the ring and dome is shown in Figure 2i. This confirms the anisotropic deformation of the PS during the RIE and DRIE processes.

Figure 3a shows the SEM images of Disks structure with different pitch and radius as indicated. H was constant at 120 nm. Figure 3b and c present the measured reflectance spectra and simulated reflectance spectra of the Disks, respectively. The simulation results were obtained using a finite-difference time-domain (FDTD) software package (FDTD Solutions, Lumerical). The material constants used for the structures in the simulation were silicon (Palik), HSQ disk (n = 1.4), PS (n = 1.67), and Al (CRC Handbook of Chemistry and Physics). A periodic boundary condition was employed, with a rectangular unit cell consisting of one whole and four quarter spheres. Other settings can be found in ref 22.

DOI: 10.1021/acsphotonics.5b00725
ACS Photonics 2016, 3, 627−633

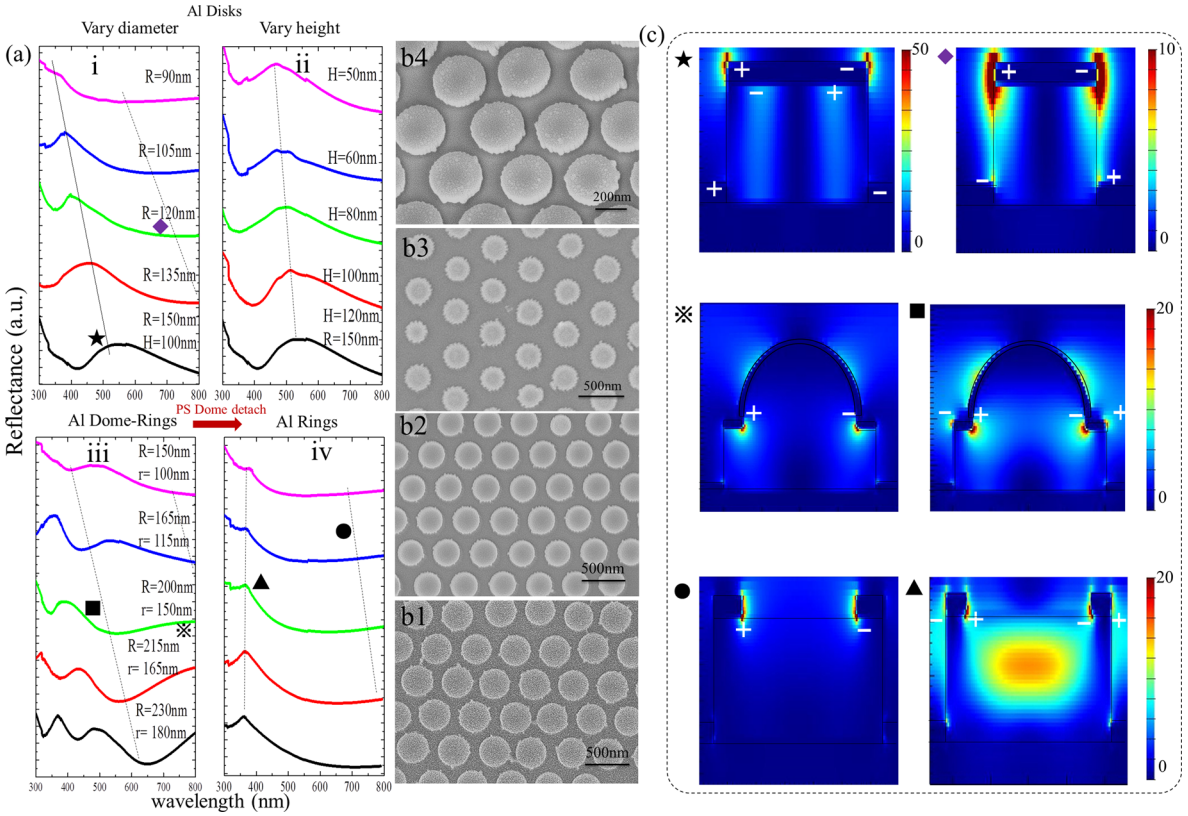

Figure 4. (a) Experimental reflectance spectra for (i) Disks with R increasing from 90 to 150 nm in 15 nm increments, P = 420 nm, H = 100 nm; (ii) Disks with H between 50 and 120 nm, P = 420 nm, R = 150 nm; (iii) Al Dome-Rings with P = 520 nm, H = 100 nm, fixed $R - r$ = 50 nm, and R between 100 and 180 nm; (iv) Rings with P = 520 nm, H = 100 nm, and fixed $(R - r)$ = 50 nm; (b) Top-view SEM images of the Disks (P = 420 nm), with R = 170 (b1), 150 (b2), and 130 nm (b3); (b4) Tilted-view SEM image with P = 420 nm, R = 150 nm, and H = 100 nm; (c) Electric field and charge distribution for various modes in Disks, Dome-Rings, and Rings corresponding to the spectra marked with symbols in (a).

Simulation results in Figure 3c show a good qualitative agreement with the measured reflectance spectra in Figure 3b. These spectra were obtained using a UV/vis system (Lambda 750S UV/Vis/NIR spectrophotometer). The reflectance curves exhibit a dominant dip that red shifts from 400 nm (a,i) to 550 nm (a,ii) and 600 nm (a,iii). The dips in the measured spectra were broader than the corresponding simulation results, likely due to ensemble averaging and higher scattering losses in the metal nanostructures. For Disks i, the reflectance peaks in the cyan and green yellow region combine to produce a pale color (Figure 3d, i and i*). For Disks ii, the reflectance peaks in the blue and red regions render a purple color (Figure 3d, ii and ii*), and for Disks iii, the dominant reflectance lies in the blue region, in agreement with the observed blue sample color (Figure 3d, iii and iii*). The corresponding chromaticity coordinates were calculated and mapped onto a standard CIE (International Commission on Illumination) 1931 chromaticity diagram,[20] as shown in Figure 3e. Good agreement was obtained between the experimental and the simulated spectra and between the measured and the calculated colors. Sample colors were captured using a digital camera under diffuse ambient lighting. These results demonstrate the feasibility of our proposed nanopatterning approach in creating large-area samples. Simulations and SEM images provide evidence that the final structures are indeed as illustrated in the process flow.

The various geometries, that is, Disks, Dome-Rings, and Rings provide a large parameter space to explore and observe the resulting colors. We systematically varied the parameters P, R, r, and H for the Al Disks, Dome-Rings, and Rings to tailor the resonances and, thus, the observed colors. Figure 4a,I shows the experimental reflectance spectra for Disks with the disk radius R ranging from 150 to 90 nm in decreasing steps of 15 nm, and P and H fixed at 420 and 100 nm. The optical response manifested a dominant reflectance peak and a dominant dip at shorter wavelengths and a broader dip at longer wavelengths (this wide dip is observable when R is small). The spectral features blue-shift as indicated by the dashed line from λ = 550 to 354 nm. Given the constant pitch, this shift indicates that local resonances instead of diffraction or propagating plasmons are responsible for the color shifts. The use of a hexagonal array allows for a factor of ~15% larger center-to-center distance than a square array before diffractive effects are observed.

Unlike structures with smaller diameters, varying the HSQ post height H here had a minimal effect on the reflectance spectra. As shown in Figure 4a, ii, the reflectance peak blue-shifts minimally from λ= 550 to 468 nm with decreasing HSQ post height H from 120 to 60 nm, with constant R = 150 nm and P = 420 nm. Figure 4b shows the representative top-view SEM images of the Disks (P = 420 nm, H = 100 nm), with decreasing R = 170 (b1), 150 (b2), and 130 nm (b3). Figure 4(b4) shows a tilt-view SEM image of one of the samples in (b2) showing the vertical sidewall profile etched into HSQ and its top-coated surface. Figure S3 shows the structures of Al Disks (P = 420 nm, R = 150 nm) with varying HSQ height of 60 (a), 90 (b) and 120 nm (c).

Due to the large pitch of the arrays used here, that is, 420, 520, and 628 nm, the colors viewed are not angle-independent. Instead, diffractive effects were evident when the samples were

DOI: 10.1021/acsphotonics.5b00725
ACS Photonics 2016, 3, 627−633

Table 1. Summarizes All the Structures Fabricated

	P = 420 nm	P = 520 nm	P = 628 nm
Al Disks		H = 50, 60, 80, 100, 120 nm	
	R = 90, 105, 120, 135 150, 180 nm	R = 100, 120, 150, 180, 210, 240 nm	R = 120, 150, 180, 210, 250 nm, 300 nm
		H = 120 nm	
Al Dome-Rings	R, r = (180, 120), (150, 100), (120, 60) nm	R, r = (250, 200), (250, 150), (230, 180), (215, 165), (200, 150), (200, 100), (180, 100), (165, 115), (150, 100) nm	R = 300, r = 250, 200; R, r = (265, 215), (250, 200), (250, 175), (250, 150), (235, 150) nm, (200, 100)
Al Rings	R, r = (150, 100), (180, 120) nm	R, r = (250, 200), (230, 180), (215, 165), (200, 150), (200, 100), (180, 100), (165, 115), (150, 100) nm	R, r = (300, 200), (250, 150), (200, 100) nm

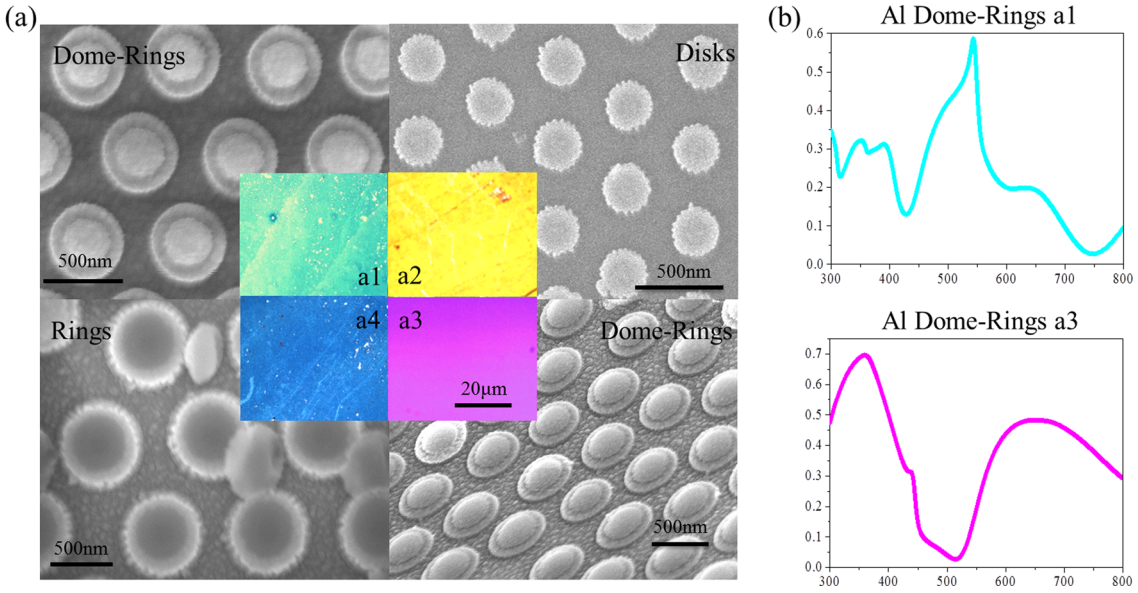

Figure 5. (a) SEM and corresponding optical microscope images showing corresponding colors for (a1) Al Dome-Rings with (P, R, r) = (628, 250, 150 nm); (a2) Disks with (P, R, H) = (420, 150, 60) nm; (a3), Al Dome-Rings with (P, R, r) = (520, 200, 100 nm); (a4) Rings with (P, R, r) = (628, 200, 100) nm; (b) Experimental reflectance spectra for Al Dome-Rings in (a1) and (a3).

viewed at off-normal angles. These effects were more apparent when either the viewing or illumination was at a glancing angle. Although diffractive effects were strongest for the larger pitch structures (i.e., 628 nm), these structures also exhibited the smallest gamut, as seen in Figure 1. Hence, diffractive effects played a small role in producing vibrant colors when viewed under normal incidence. As we focus our attention to normal-incidence illumination and viewing, detailed characterization of these diffractive effects will be a topic for future investigations.

Using the same approach as in Figure 3d, we map the reflectance curves of the various Al Disks onto the CIE chromaticity diagram, as shown in Figure 1 by the red (P = 628 nm series), orange (P = 520 nm series), and black symbols (P = 420 nm series), connected by the corresponding color lines. We found that colors from the Al Disks for P = 628 nm, 520 nm series are located in the bluish region, whereas colors from the P = 420 nm series exhibited the largest gamut, spanning the light blue, yellow, yellow green, and pink regions. The larger gamut occupied by smaller pitch structures suggests that diffractive effects typically seen at larger pitch were not effective in enhancing the color saturation.

The Al Dome-Rings structure exhibits complex plasmon resonances due to the coupling between modes of the dome and ring structures. These hybrid modes are observed as multiple dips and peaks in the reflectance spectra. At a fixed pitch, the modes are determined by the outer radius R and inner radius r. As shown in Figure 4a, iii, with P = 520 nm, H = 100 nm, and fixed $R - r$ = 50 nm, the number of peaks decreases and the peaks blueshift with decreasing R, that is, three dips for R = 230 nm and one dip for R = 150 nm. This behavior is consistent with the decreasing number of high order modes that can be supported as the nanostructure size decreases. The reflectance recovers to resemble that of the corresponding Disks when R was shrunk to be as small as 165 nm (r = 115 nm), suggesting that the domes and rings have merged to form a disk-like structure.

The Rings structure was obtained by sonicating the Al Dome-Rings structure to remove the top dome. The Rings structure shows a rather distinct reflectance curve compared to the other structures. Figure 4a, iv shows the reflectance of the Rings with the same outer and inner radii as the Al Dome-Rings in Figure 4a, iii, that is, with a constant $R - r$ = 50 nm. Note that the peaks and dips present in the Al Dome-Rings reflectance spectra are absent in the spectra of the Rings, indicating the removal of the hybridized modes. Instead, the reflectance of the Rings shows a dominant peak at short wavelengths (~363 nm for R, r = 230, 180 nm) and a wide dip at longer wavelengths. This peak is due to the localized mode supported across the 50 nm wide ring, as indicated by the corresponding field distribution. As shown by the blue hexagonal symbols in Figure 1, this resonance extends the gamut to the deep blue region.

We performed FDTD simulations to scrutinize the underlying mechanism governing the reflectance response of Al

DOI: 10.1021/acsphotonics.5b00725
ACS Photonics 2016, 3, 627−633

Disks, Dome-Rings, and Rings. Figure 4c shows the electric field and indicated charge distributions of the dominant modes for Al Disks (upper panel), Dome-Rings (middle panel), and Rings (bottom panel). For the previously reported Disks structure for color generation,[2] it is the fundamental mode (denoted by purple diamonds, also see the Supporting Information, Figure S4.2) that dominates the spectrum in the visible range. In contrast, the high order mode (black star) dominates in our Al Disks due to the relatively larger size of the structures.[24] A broad dipole bonding resonance and a relatively narrow anti-bonding-like resonance are excited at the Al Rings at the long and short wavelength sides, respectively, as shown by the electric intensity and charge distribution in the bottom panel of Figure 4c. More discussions and analysis on the spectra of Al Disks, Dome-Rings and Rings can be found in the Supporting Information, Figures S4–6.

Table 1 summarizes all the Disks, Dome-Rings, and Rings structures fabricated. Figure 5a shows the SEM and corresponding optical micrographs for the most vibrant color palettes achieved in the range of parameters studied. Figure 5(a2) shows the SEM image of the Disks with $(P, R, H) = (420, 150, 60)$ nm, and the corresponding vibrant yellow color image (left bottom corner in Figure 5(a2)). Figure 5a1 and a3 show the SEM images of the Al Dome-Rings, with $(P, R, r) = (628, 250, 150)$ nm and $(520, 200, 100)$ nm, respectively. The corresponding colors are light green and pink, as shown by the color images, with coordinates (0.20, 0.396) and (0.386, 0.267) on the CIE map. The introduction of multiple structures, that is, the Dome-Ring, creates multiple local resonances that couple to produce the sharp spectral features shown. While a more detailed analysis of the coupling mechanism is beyond the scope of this report, the results indicate that one can potentially use multiple structures with complex resonances to create sharper spectral features that could lead to a broader color gamut. The removal of the PS dome structure and the corresponding featureless spectra of the Rings structure support this claim.[23,24] Figure 5(a4) shows the SEM image of the Rings with $(P, R, r) = (628, 250, 150)$ nm, which is correlated with microscope color images representing the deep blue color.

CONCLUSION

We have successfully fabricated hexagonal arrays of Al Disks, Dome-Rings, and Rings structures using the colloidal self-assembly approach. Large area aluminum plasmonic color palettes with an expanded gamut were obtained by systematically adjusting the structural parameters, including the periodicity (P), radius (R, r), and height (H). The Disks with 420 nm pitch show the largest gamut, spanning yellow, pink, and light blue. Conversely, the Disks with 628 nm pitch shows the smallest gamut, mainly located in the light blue region. Ring structures were effective in producing deep blue colors. Localized modes of the PS dome are incorporated to increase the color gamut further in the Al Dome-Rings. Resonant modes obtained through simulations indicate the complex coupling between the different structures that could be used to sharpen the reflectance spectra. The hexagonal array used permitted larger diameter structures to be used. These structures can support a higher-order resonance mode than previously reported. This work provides an approach for rapid evaluation of plasmonic colors followed by simulations for selected parameters to extract the underlying resonances.

ASSOCIATED CONTENT

Supporting Information

The Supporting Information is available free of charge on the ACS Publications website at DOI: 10.1021/acsphotonics.5b00725.

Figure S1 shows that surface irregularities and roughness appeared during PS shrinkage and were transferred to the HSQ Disks after etching; Figure S2 shows our sample with a large uniformly patterned area over 120 μm by 100 μm; Figure S3 shows the structures of Disks (P = 420 nm, R = 150 nm) with varying HSQ height; Figures S4, S5, and S6 provide discussion and analysis of the resonances modes in Disks, Dome-Rings, and Rings (PDF).

AUTHOR INFORMATION

Corresponding Author

*E-mail: joel_yang@sutd.edu.sg.

Notes

The authors declare no competing financial interest.

ACKNOWLEDGMENTS

This work was supported by the SUTD-MIT International Design Centre Grant No. IDG31400113 and the SUTD Digital Manufacturing and Design (DManD) Centre Grant No. RGDM1530302.

REFERENCES

(1) Abbe, E. A. Contribution to the theory of the microscope and the nature of microscopic vision. *Proc. Bristol Nat. Soc.* **1874**, *1*, 200–261.

(2) Kumar, K.; Duan, H.; Hegde, R. S.; Koh, S. C.; Wei, J. N.; Yang, J. K. Printing colour at the optical diffraction limit. *Nat. Nanotechnol.* **2012**, *7* (9), 557–561.

(3) Roberts, A. S.; Pors, A.; Albrektsen, O.; Bozhevolnyi, S. I. Subwavelength plasmonic color printing protected for ambient use. *Nano Lett.* **2014**, *14* (2), 783–787.

(4) Tan, S. J.; Zhang, L.; Zhu, D.; Goh, X. M.; Wang, Y. M.; Kumar, K.; Yang, J. K. Plasmonic color palettes for photorealistic printing with aluminum nanostructures. *Nano Lett.* **2014**, *14* (7), 4023–4029.

(5) Clausen, J. S.; Højlund-Nielsen, E.; Christiansen, A. B.; Yazdi, S.; Grajower, M.; Taha, H.; Mortensen, N. A. Plasmonic metasurfaces for coloration of plastic consumer products. *Nano Lett.* **2014**, *14* (8), 4499–4504.

(6) Ozaki, M.; Kato, J. I.; Kawata, S. Surface-plasmon holography with white-light illumination. *Science* **2011**, *332* (6026), 218–220.

(7) Shrestha, V. R.; Lee, S. S.; Kim, E. S.; Choi, D. Y. Aluminum plasmonics based highly transmissive polarization-independent subtractive color filters exploiting a nanopatch array. *Nano Lett.* **2014**, *14* (11), 6672–6678.

(8) Ellenbogen, T.; Seo, K.; Crozier, K. B. Chromatic plasmonic polarizers for active visible color filtering and polarimetry. *Nano Lett.* **2012**, *12* (2), 1026–1031.

(9) Laux, E.; Genet, C.; Skauli, T.; Ebbesen, T. W. Plasmonic photon sorters for spectral and polarimetric imaging. *Nat. Photonics* **2008**, *2* (3), 161–164.

(10) Goh, X. M.; Zheng, Y.; Tan, S. J.; Zhang, L.; Kumar, K.; Qiu, C. W.; Yang, J. K. Three-dimensional plasmonic stereoscopic prints in full color. *Nat. Commun.* **2014**, *5*, 5361.

(11) Olson, J.; Manjavacas, A.; Liu, L.; Chang, W. S.; Foerster, B.; King, N. S.; Link, S. Vivid, full-color aluminum plasmonic pixels. *Proc. Natl. Acad. Sci. U. S. A.* **2014**, *111* (40), 14348–14353.

(12) Inoue, D.; Miura, A.; Nomura, T.; Fujikawa, H.; Sato, K.; Ikeda, N.; Koide, Y. Polarization independent visible color filter comprising an aluminum film with surface-plasmon enhanced transmission

DOI: 10.1021/acsphotonics.5b00725
ACS Photonics 2016, 3, 627–633

through a subwavelength array of holes. *Appl. Phys. Lett.* **2011**, *98* (9), 093113.
(13) King, N. S.; Liu, L.; Yang, X.; Cerjan, B.; Everitt, H. O.; Nordlander, P.; Halas, N. J. Fano Resonant Aluminum Nanoclusters for Plasmonic Colorimetric Sensing. *ACS Nano* **2015**, *9* (11), 10628−10636.
(14) Duempelmann, L.; Casari, D.; Luu-Dinh, A.; Gallinet, B.; Novotny, L. Color Rendering Plasmonic Aluminum Substrates with Angular Symmetry Breaking. *ACS Nano* **2015**, *9*, 12383.
(15) Ye, X.; Qi, L. Two-dimensionally patterned nanostructures based on monolayer colloidal crystals: controllable fabrication, assembly, and applications. *Nano Today* **2011**, *6* (6), 608−631.
(16) Bardosova, M.; Pemble, M. E.; Povey, I. M.; Tredgold, R. H. The Langmuir-Blodgett Approach to Making Colloidal Photonic Crystals from Silica Spheres. *Adv. Mater.* **2010**, *22* (29), 3104−3124.
(17) Im, H.; Bantz, K. C.; Lee, S. H.; Johnson, T. W.; Haynes, C. L.; Oh, S. H. Self-Assembled Plasmonic Nanoring Cavity Arrays for SERS and LSPR Biosensing. *Adv. Mater.* **2013**, *25* (19), 2678−2685.
(18) Lee, S. H.; Bantz, K. C.; Lindquist, N. C.; Oh, S. H.; Haynes, C. L. Self-assembled plasmonic nanohole arrays. *Langmuir* **2009**, *25* (23), 13685−13693.
(19) https://en.wikipedia.org/wiki/Gamut; http://www.prweb.com/releases/Smallhd/OLED/prweb10177557.htm.
(20) CIE Technical Report. *Colorimetry*, 3rd ed., CIE 15:2004; Commission Internationale de l'Eclairage: Vienna, Austria, 2004.
(21) Vogel, N.; Goerres, S.; Landfester, K.; Weiss, C. K. A Convenient Method to Produce Close-and Non-close-Packed Monolayers using Direct Assembly at the Air−Water Interface and Subsequent Plasma-Induced Size Reduction. *Macromol. Chem. Phys.* **2011**, *212* (16), 1719−1734.
(22) Ng, R. J. H.; Goh, X. M.; Yang, J. K. All-Metal Nanostructured Substrates as Subtractive Color Reflectors with Near-Perfect Absorptance. *Opt. Express* **2015**, *23* (25), 32597−32605.
(23) Romanov, S. G.; Korovin, A. V.; Regensburger, A.; Peschel, U. Hybrid Colloidal Plasmonic-Photonic Crystals. *Adv. Mater.* **2011**, *23* (22−23), 2515−2533.
(24) Maier, S. A. *Plasmonics: Fundamentals and Applications*; Springer Science & Business Media, 2007.

DOI: 10.1021/acsphotonics.5b00725
ACS Photonics 2016, 3, 627−633